

⁹The exact expressions are

$$\begin{aligned}
 C_{2,2}{}^{n,i} &= \frac{\gamma_n^{(0)}}{2\beta_0^3} \beta_1^2 \left(1 + \frac{\gamma_n^{(0)}}{2\beta_0} \right); \\
 C_{2,1}{}^{n,i} &= \frac{\gamma_n^{(0)}}{2\beta_0^3} \beta_1^2 + \frac{\beta_1}{\beta_0} \left(1 + \frac{\gamma_n^{(0)}}{2\beta_0} \right) \\
 &\quad \times \left[c_i{}^{n(1)} + \frac{1}{2\beta_0} \left(\gamma_n^{(1)} - \frac{\beta_1}{\beta_0} \gamma_n^{(0)} \right) \right]; \\
 C_{2,0}{}^{n,i} &= \frac{1}{4\beta_0} \left(\gamma_n^{(2)} + \frac{\beta_2}{\beta_0} \gamma_n^{(0)} - \frac{\beta_1}{\beta_0} \gamma_n^{(1)} - \frac{\beta_1^2}{\beta_0^2} \gamma_n^{(0)} \right) \\
 &\quad + \frac{1}{8\beta_0^2} \left[\gamma_n^{(1)2} - 2\gamma_n^{(1)} \frac{\beta_1}{\beta_0} \gamma_n^{(0)} + \left(\frac{\beta_1}{\beta_0} \right)^2 \gamma_n^{(0)2} \right] \\
 &\quad + c_i{}^{n(1)} \frac{1}{2\beta_0} \left(\gamma_n^{(1)} - \frac{\beta_1}{\beta_0} \gamma_n^{(0)} \right) + c_i{}^{n(2)}.
 \end{aligned}$$

We give these expressions here since $C_{2,2}{}^{n,i}$ had a typing error in Ref. 7.

¹⁰R. C. Brower, M. A. Furman, and M. Moshe, Phys. Lett. **B76**, 213 (1978). In this calculation the quality of the estimate had been checked when compared to the exactly calculated next-order term. Since the high-temperature series had been calculated to a high order (20 orders in $D=1$ and 10 orders in $D=2$) it serves as a good laboratory for checking such and other approximate estimates which can be tested repeatedly.

¹¹M. Moshe, to be published. Some differences can be seen when comparing the results obtained in the

renormalization scheme used here (Ref. 7) to those obtained in the renormalization scheme of Ref. 2 (the \overline{MS} scheme) but they both point to very similar conclusions.

¹²Comparing the estimate of the two-loop contribution versus the estimate of the three-loop contribution one observes that the error in the former is somewhat larger at low q^2 . Indeed, it is so and the reason is that in the two-loop contribution in Fig. 2 the terms $C_{1,0}{}^{4,i}$ and $C_{1,1}{}^{4,i} \ln g_0^2$ come out with opposite signs. This property brings much instability to $C_i{}^{4(q^2/\Lambda^2)}$ while $C_{1,0}{}^{4,i}$ is varied. In the order- g_0^4 part, there are three coefficients contributing ($C_{2,j}{}^{4,i}$, $j=0,1,2$) and no such instabilities are found. Note that altogether only three out of twenty terms are unknown in the order g_0^4 contribution.

¹³R. Barbieri, L. Caneschi, R. Curci, and E. d'Emilio, Phys. Lett. **81B**, 207 (1979).

¹⁴Note that one can further push the estimate to the order g_0^6 term. Here the terms $C_{3,3}{}^{n,i} \ln^3 g_0^2$ and $C_{3,2}{}^{n,i} \ln^2 g_0^2$ are exactly known from the two-loop results but $C_{3,1}{}^{n,i} \ln g_0^2$ and also $C_{3,0}{}^{n,i}$ are only partially known and thus the error is increasing at this stage.

¹⁵As to the much discussed $\gamma\gamma$ process, the third-loop contribution to the calculable structure function $F_2^\gamma(x, q^2)$ is of order $(\ln q^2)^{-1}$ and thus competes with the uncalculable part from the hadronic matrix element making it hard for detection.

¹⁶T. Kinoshita, Nuovo Cimento **51B**, 140 (1967).

¹⁷B. Lautrup and E. de Rafael, Nucl. Phys. **B70**, 317 (1979).

Optical Isomer Shift for the Spontaneous-Fission Isomer $^{240}\text{Am}^m$

C. E. Bemis, Jr., J. R. Beene, J. P. Young, and S. D. Kramer

Oak Ridge National Laboratory, Oak Ridge, Tennessee 37830

(Received 9 October 1979)

The optical isomer shift in the $^8S_{7/2} \rightarrow ^{10}P_{7/2}$ atomic transition in neutral americium has been measured for the ~ 1 -ms spontaneously fissioning isomer, $^{240}\text{Am}^m(\text{SF})$. With use of a laser-excited optical pumping technique, this transition is shifted by $+2.6 \pm 0.2 \text{ \AA}$ to $6407.2 \pm 0.2 \text{ \AA}$ implying a difference in nuclear mean square radii, $\delta \langle r^2 \rangle$, of $5.1 \pm 0.2 \text{ fm}^2$ between the fission isomer and the normal ground state. These experiments provide the first direct experimental proof for the large deformations expected for fission isomers.

Studies of spontaneously fissioning isomers, discovered in the early 1960's, have led to a better understanding of the detailed nature of the nuclear potential energy surface at large deformations.¹ Fission isomers are presumably shape isomers existing in a secondary minimum in the potential energy surface at approximately twice the quadrupolar deformation of the normal nuclear ground states of nuclei in the actinide region.¹ Until recently, detailed knowledge of fission isomeric states has been mostly limited to half-

lives and excitation energies; the static nuclear properties are poorly known because of the difficulty in producing and studying these short-lived isomers. From conversion-electron studies,²⁻⁴ from rotational band feeding and decay times using the charge-plunger method,^{5,6} and from delayed-fission fragment angular distributions,⁷ indirect but consistent evidence for large deformations has been obtained. Inferred intrinsic quadrupole moments, Q_0 , range from 25 to 35 b, as expected for fission isomers.

Optical isotope shifts in atomic line spectra provide a very sensitive measure of deviations of the nuclear charge distribution from spherical symmetry. Indeed, the anomalously large isotope shifts in the optical spectra of the rare earth elements provided some of the earliest direct evidence for the large static quadrupolar deformation for nuclides in this mass region.⁸ In this Letter, we report the determination of the optical isomer shift for the fission-isomeric state of ^{240}Am which is the first direct measure of the rms radius change, $\delta\langle r^2 \rangle$, between the normal americium ground state and the fission-isomeric state. This measurement, therefore, provides a direct experimental proof for the extremely large nuclear deformation commonly assumed for the fission-isomeric states.

We have developed an in-beam laser-excited optical pumping technique to achieve dynamic nuclear orientation and to perform high-resolution optical spectroscopy on accelerator-produced, short-lived nuclides. This technique, called LINUP (Laser-Induced Nuclear Polarization), is based on depopulation optical pumping⁹ with circularly polarized light (σ_+ or σ_-). When completed, the optical pumping cycle results in an orientation of the total angular momentum, $\vec{F} = \vec{I} + \vec{J}$, in the atomic ground state. Here, I and J are the nuclear and atomic spins, respectively; and the projections of F , I , and J on an external reference axis, the laser beam propagation axis in this case, are $M_{F,I,J}$. The optical pumping cycle consists of resonant absorption with the selection rule $\Delta M_F = +1$ for σ_+ light, followed by spontaneous radiative decay with the selection rule $\Delta M_F = 0, \pm 1$. Subsequent spontaneous-fission decay from the oriented nuclear system is anisotropic, if the nuclear spin $I \neq 0$ or $\frac{1}{2}$, and the anisotropic decay is the signal for the optical resonance condition. The LINUP method is similar in principle to that proposed by Burns *et al.*¹⁰ and to the radiation-detected optical pumping technique.^{11,12}

Americium is a good candidate for optical pumping because the ground state, $5f^7 7s^2 \ ^8S_{7/2}$, has approximate spherical symmetry which reduces collisional relaxation and because the first excited state arises from the promotion of one $7s$ electron to the $7p$ orbital, $5f^7 7s 7p \ ^{10}P_{7/2}$. The hyperfine structure states associated with the $^8S_{7/2}$ ground state are nearly degenerate¹³ ($\leq 0.001 \text{ cm}^{-1}$) and the hyperfine states associated with the $^{10}P_{7/2}$ state are contained within a band of 0.4 \AA for the $6405\text{-\AA} \ ^{10}P_{7/2} \rightarrow \ ^8S_{7/2}$ transition in either ^{241}Am or

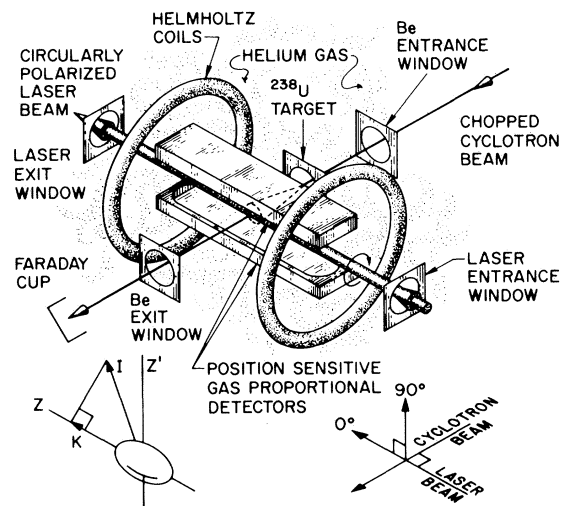


FIG. 1. Schematic of the optical pumping cell showing the geometrical arrangement of the position-sensitive detectors, the laser beam, and cyclotron beam. The laser and cyclotron beams are both 0.4 cm in diameter.

^{243}Am . The total width should be $\sim 0.5 \text{ \AA}$ for reasonable choices of I and g_I for the fission isomer $^{240}\text{Am}^m$. In the absence of atomic ground-state relaxation, laser optical pumping with σ_+ light, with a bandwidth greater than the total width of the $^{10}P_{7/2}$ hyperfine structure, ultimately results in the population of the ground-state level with $F_{\text{max}} = \frac{7}{2} + I$ and sublevel $M_F = +F_{\text{max}}$ from which no further laser absorptions may occur. The system, both atomic and nuclear, is then totally polarized.

The $^{240}\text{Am}^m$ fission isomer was selected for our first LINUP experiments. For this case, the nuclear lifetime ($\sim 1 \text{ ms}$) is long compared to the radiative lifetime¹⁴ for the $^{10}P_{7/2}$ state ($\sim 2 \text{ \mu s}$) and short compared to the estimated diffusion times for Am atoms out of the laser beam volume. The arrangement of the optical pumping cell is shown schematically in Fig. 1. The $^{240}\text{Am}^m$ was produced in the reaction $^{238}\text{U}(^7\text{Li}, 5n)$ with 49.0-MeV $^7\text{Li}^{+2}$ ions from the Oak Ridge isochronous cyclotron. After passage through the entrance window and the 0.9-mg/cm² Ni target backing, the ^7Li beam energy was degraded to $\sim 47.5 \text{ MeV}$, an energy which corresponds to our measured maximum $^{240}\text{Am}^m$ production cross section of $1.8 \pm 0.1 \text{ \mu b}$. Fission-isomeric recoils rejected from the UO_2 target (30 \mu g U/cm^2) were thermalized in 180 Torr of helium gas. The peak of the distribution of thermalized recoils was located 15.5 mm downstream, along the long position-sensing axis of two gas proportional detectors (PSPD). The

PSPD's, each 60 mm long \times 8 mm wide, were located above and below the reaction plane and each detector subtended a solid angle of 12.5% of 4π steradians for decay events originating in mid-counter on the detector axis.

A σ_+ continuous-wave laser beam, perpendicular to the cyclotron beam and along the long axis of the PSPD's, was focused to a diameter of 0.4 cm at the location of the thermalized recoils. The laser power density at this location was ≥ 5 W cm^{-2} and the tunable laser output linewidth was restricted to ~ 0.5 Å with use of an intracavity birefringent filter. The degree of circular polarization, σ_+/σ_- , was greater than 2000:1. The laser wavelengths were established to an accuracy of 0.02 Å relative to the 6402.246-Å line in NeI using a 1.5-m double-pass monochromator. A small magnetic "keeper" field, ~ 3 G, was produced along the laser beam propagation axis by means of a Helmholtz-coil pair to preserve the orientation of oriented atoms.

The ${}^7\text{Li}$ cyclotron beam was mechanically chopped to provide equal 2-ms beam-off and beam-on periods and data were recorded during the beam-off period. About 200 single-fragment decay events from ${}^{240}\text{Am}^m$, forty of which are fast coincidence events between the PSPD's, were recorded per hour at a beam current of 2 μA . The laser output wavelength was scanned in the interval 6406–6410 Å using 0.25-Å steps. At each step, data were recorded for an integrated ${}^7\text{Li}$ beam current of 10 mC. Four scans of the 4-Å interval were completed for the experiments described

here.

Anisotropic spontaneous-fission decay from the oriented nuclear system with $K=I=|M_I|$, as would be achieved in our experiments, preferentially occurs along the laser beam propagation axis at 0° , with the anisotropy $W(0^\circ)/W(90^\circ)$ given by 2^{2K-1} (see e.g., Fraser and Milton¹⁵). The solid angle per unit length along the PSPD's is largest for events that occur at 90° with respect to the laser beam propagation axis and one obvious manifestation of anisotropic fission decay is a decrease in coincident fission-event yield for the middle sections of the PSPD's. We show this coincident event yield, normalized to integrated beam current, as a function of laser wavelength in Fig. 2(a). A decrease in yield, i.e., anisotropic fission decay, is evident at a wavelength of 6407.7 ± 0.2 Å. This effect was apparent in three of the four wavelength scans but the magnitude of the effect decreased between successive scans. No statistically significant effect was observed in the fourth scan. The four scans took a total of 112 h to complete and we speculate that sufficient ${}^7\text{Li}$ atoms and other impurities were present in the cell at the completion of the experiments to diminish any orientation of the Am system by the spin-exchange relaxation mechanism.⁹

The weighted average coincidence fission yield per millicoulomb off resonance is 2.84 ± 0.12 and the yield at 6407.7 Å is 1.84 ± 0.35 . We are unable to extract statistically significant fission-fragment angular distributions using the position information from our PSPD's. A large fraction of

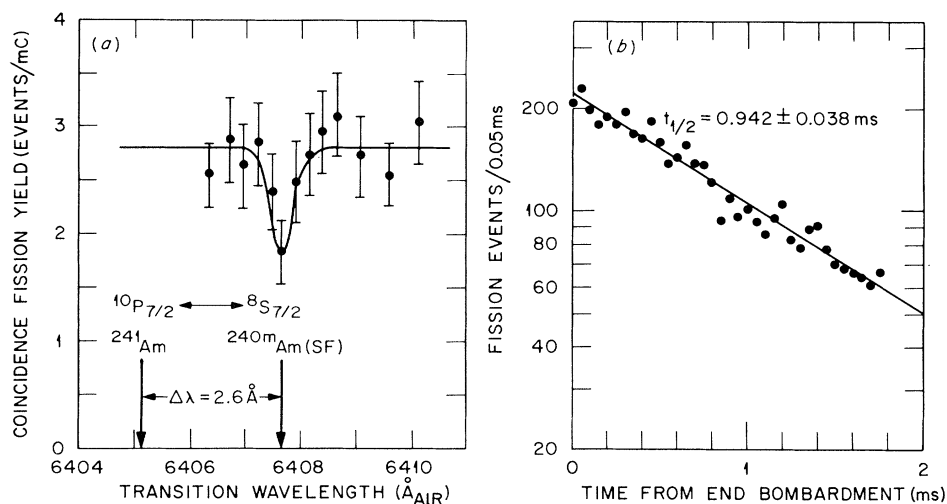


FIG. 2. (a) Normalized fission-fragment coincidence yield as a function of laser wavelength. The decrease in yield at 6407.7 Å indicates anisotropic fission decay due to orientation via resonant optical pumping. The solid curve is shown to guide the eye. (b) The decay of fission events relative to the end of a beam-on cycle. The single-component decay is due to ${}^{240}\text{Am}^m(\text{SF})$.

fission-fragment events comprise an isotropic background which arises either because of relaxation effects, or because the atoms are outside the laser beam volume or cannot be optically pumped since they remain as ions in the thermalization process.

The time distribution for the fission events, measured from the end of a beam-on period, is shown in Fig. 2(b). These data are best fitted with a single-component exponential decay with a half-life of 0.942 ± 0.038 ms. No evidence for additional decay components was found in these experiments. Other determinations of the half-life for $^{240}\text{Am}^m$, compiled by Schmorak,¹⁶ overlap our more accurate value. Since no other spontaneous-fission activities¹⁷ in the U, Np, Pu, Am region have half-lives of ~ 1 ms except $^{240}\text{Am}^m$, together with the agreement in incident ^7Li energy for our measured peak cross section with values calculated¹⁸ for the reaction $^{238}\text{U}(^7\text{Li}, 5n)$, the assignment of fission events to the decay of $^{240}\text{Am}^m$ is assured.

The $^8\text{S}_{7/2} \rightarrow ^{10}\text{P}_{7/2}$ transition in ^{241}Am occurs at a wavelength¹³ of 6405.105 \AA and is shifted to longer wavelength by 0.09685 \AA when this transition occurs in ^{243}Am . The isotope or isomer shifts in heavy elements like americium arise predominantly from the volume effect, a change in overlap of the nuclear and electronic charge distributions from one isotope or isomer to another. This volume or field shift is customarily expressed¹⁹ as the product of a purely electronic factor and a nuclear factor, $\Delta\nu = F \delta\langle r^2 \rangle$, where $\Delta\nu$ is the shift in transition frequency or wave number of an atomic spectral line. Here F is the purely electronic factor, proportional to the change in total relativistic electron charge density at the nucleus, $\Delta|\psi(0)|^2$, in the atomic transition and, for a given atomic transition, has the same value for all isotopes or isomers of the same element. The nuclear factor, $\delta\langle r^2 \rangle$, is the change in mean square radii of the nuclear charge distributions between the isotopic or isomeric pair. Higher radial nuclear charge moments yield terms proportional to $\delta\langle r^N \rangle$, where $N > 2$, but these terms are negligible for our purposes.²⁰ Since the electronic factor, F , for the $^8\text{S}_{7/2} \rightarrow ^{10}\text{P}_{7/2}$ transition is expected to be the same for $^{240}\text{Am}^m$ as for ^{241}Am and ^{243}Am , we directly derive from the experimental shifts $\delta\langle r^2 \rangle_{240m-241} = (26.8 \pm 2.0)\delta\langle r^2 \rangle_{243-241}$. This result, independent of any nuclear or atomic model assumptions, indicates a very large nuclear deformation for the spontaneous fission isomer $^{240}\text{Am}^m$.

From the extensive analysis of Rajnak and

Fred,²¹ we take the $^{241-243}\text{Am}$ isotope shift to be due entirely to a change in $\langle r^2 \rangle$ which is adequately accounted for in terms of the mass number A by the parametrization²²

$$\langle r^2 \rangle = \langle r^2 \rangle_0 [1 + (5/4\pi)\beta^2], \quad (1)$$

where $\langle r^2 \rangle_0$ is the mean square radius of the charge distribution for a spherical nucleus given by $\langle r^2 \rangle_0 = [(3/5)^{1/2} r_0 A^{1/3}]^2$ and β is the quadrupole deformation parameter. Using Eq. (1) and our result for $\delta\langle r^2 \rangle_{240m-241}$, we obtain $\delta\langle r^2 \rangle = 5.1 \pm 0.2 \text{ fm}^2$ between the ground-state isomer ^{240}Am and the spontaneous-fission isomer $^{240}\text{Am}^m$. We have used $r_0 = 1.2 \text{ fm}$ and have taken the quadrupole deformation parameter²³ $\beta = 0.24$ for ^{240}Am , ^{241}Am , and ^{243}Am . The uncertainty in $\delta\langle r^2 \rangle_{240m-240}$ allows for an odd-even staggering in the isotope shift for the Am isotopes twice as large as those observed for the neighboring actinides.²¹ Using Eq. (1), we also derive a quadrupole deformation parameter β of 0.66 ± 0.04 for the fission-isomeric state. The deduced intrinsic quadrupole moment, Q_0 , is $32.7 \pm 2.0 \text{ b}$ from the relation $Q_0 = [3Z\langle r^2 \rangle / (5\pi)^{1/2} [\beta(1 + 0.36\beta)]]$ which corresponds to a prolate spheroid with a major-to-minor axis ratio of $\sim 2:1$.

In summary, we have measured the optical isomer shift for the spontaneously fissioning isomer, $^{240}\text{Am}^m$. The extremely large value of 5.1 fm^2 for $\delta\langle r^2 \rangle$ suggests a large change in deformation between the fission-isomeric state and the normal ground state. The deduced deformation parameter, $\beta = 0.66 \pm 0.04$, and intrinsic quadrupole moment, $Q_0 = 32.7 \pm 2.0 \text{ b}$, are in agreement with the values expected²⁴ for fission isomers near $A = 240$ and *this experiment provides the first direct experimental proof for these large deformations*.

This work is supported by the Division of High Energy and Nuclear Physics, Office of Energy Research, U. S. Department of Energy, under Contract No. W-eng-26-7405 with Union Carbide Corporation.

¹R. Vandenbosch, *Annu. Rev. Nucl. Sci.* **27**, 1 (1977).

²H. J. Specht *et al.*, *Phys. Lett.* **41B**, 43 (1972).

³J. Borggreen *et al.*, *Nucl. Phys.* **A279**, 189 (1977).

⁴H. Backe *et al.*, *Phys. Rev. Lett.* **42**, 490 (1979).

⁵D. Habs *et al.*, *Phys. Rev. Lett.* **38**, 387 (1977).

⁶G. Ulfert *et al.*, *Phys. Rev. Lett.* **42**, 1596 (1979).

⁷V. Metag and G. Sletten, *Nucl. Phys.* **A282**, 77 (1977).

⁸P. Brix and A. Kopfermann, *Z. Phys.* **126**, 344 (1949), and *Rev. Mod. Phys.* **30**, 317 (1958).

⁹W. Happer, *Rev. Mod. Phys.* **44**, 169 (1972).

- ¹⁰M. Burns *et al.*, Nucl. Instrum. Methods 141, 429 (1977); first experimental results are reported by M. S. Feld and D. E. Murnick, in *Laser Spectroscopy IV*, edited by H. Walther and K. W. Rothe (Springer-Verlag, Berlin, 1979), p. 549.
- ¹¹U. Köpf *et al.*, Z. Phys. 244, 297 (1971).
- ¹²U. Capeller and W. Mazurkewitz, J. Magn. Res. 10, 15 (1973).
- ¹³M. Fred and F. S. Tomkins, J. Opt. Soc. Am. 47, 1076 (1957).
- ¹⁴In analogy with EuI for which radiative lifetimes have been determined; V. A. Komorovskii *et al.*, Opt. Spektrosk. 25, 155 (1968) [Opt. Spectrosc. 25, 81 (1968)].
- ¹⁵J. S. Fraser and J. C. D. Milton, Annu. Rev. Nucl. Sci. 16, 379 (1966).
- ¹⁶M. R. Schmorak, Nucl. Data Sheets 20, 165 (1977).
- ¹⁷W. B. Ewbank *et al.*, Nucl. Data Sheets 26, 1 (1979).
- ¹⁸T. Sikkeland *et al.*, Phys. Rev. 172, 1232 (1968).
- ¹⁹K. Heilig and A. Steudel, At. Data Nucl. Data Tables 14, 613 (1974).
- ²⁰H. C. Seltzer, Phys. Rev. 188, 1969.
- ²¹K. Rajnak and M. Fred, J. Opt. Soc. Am. 67, 1314 (1977).
- ²²A. Bohr and B. R. Mottelson, *Nuclear Structure* (Benjamin, New York, 1969), Vol. 1, pp. 158–165.
- ²³R. R. Chasman *et al.*, Rev. Mod. Phys. 49, 833 (1977).
- ²⁴M. Brack *et al.*, Nucl. Phys. A234, 185 (1974).